DUAL MODE FRACTURE OF COMPOSITE LAMINATES PENETRATED BY SPHERICAL PROJECTILES

G. J. Czarnecki
Wright Laboratory
Wright-Patterson AFB, Ohio

Abstract

The basis for delamination initiation and propagation within an impacted laminate was studied, with an explanation provided for the fracture mode transformation along the projectile's path. Post-impact observations of graphite/epoxy (AS4/3501-6) laminates penetrated by steel spheres (0.5-inch diameter) reveal a fracture mode, similar to shear plugging, adjacent to the impacted surface. This fracture mode is contrasted with that of delamination adjacent to the rear surface. The sudden transition from shear plugging to delamination is believed to occur when the projectile interacts with the returning impact-generated tensile wave. To demonstrate the transition, results are presented from ballistically impacted laminates containing a series of imbedded carbon stress and constantan strain gages. Results are based on impact velocities of 1300, 1850, and 2380 f/s. Transverse stress waves are shown capable of creating delamination until attenuated by a local zone of compressed material associated with the on-coming projectile. Based on experimental results, the location of the fracture mode transition plane is predicted both graphically and through a simple equation of motion.

I. Introduction

Composites absorb significant amounts of impact energy through fracture events rather than by elastic or plastic deformations as do metals[1]. The damage state depends on structural geometry, boundary conditions, stacking sequence, material properties, impact energy, and impactor geometry[2]. Poor laminate out-of-plane mechanical properties allow kinetic energy from any source (dropped tools or missile warhead fragments) to cause a combination of damage in the form of delamination, transverse matrix cracking, fiber fracture, and fiber-matrix interface disbonds. During severe impacts, laminates typically sustain all four modes of fracture. The predominance of each type of damage depends on the lay-up, thickness, and impact energy[1]. Fiber fracture is the primary means by which tensile properties are reduced[3], whereas delamination is the principal mechanism by which compression properties are degraded[2].

Understanding the low velocity impact problem requires a knowledge of contact behavior, elastic wave propagation, and crack nucleation/propagation. Significant fracture (involving through-the-thickness penetration and delamination several times the projectile's diameter) enters into the high velocity impact problem and requires a more in-depth understanding of fracture mechanisms. Damage tolerance cannot be fully achieved without a complete understanding of fracture mechanisms and means of attenuation.

Numerous damage theories exist. Several researchers discuss lamina stiffness mismatches as a primary factor leading to delamination. Some researchers believe cracking and delamination are the result of flexure, whereas others suggest shear forces generated during impact lead to matrix cracking and subsequent delamination. One group of researchers believes damage is propagated mechanically (from front to rear) via a generator strip. Conversely, other researchers[4-7] propose that through-the-thickness tensile forces create delamination beginning at the rear surface and propagating toward the impacted surface.

Foos[4] suggested rear face delamination was the result of a tensile stress wave (a reflected compression wave) and experimentally observed delamination initiating on the rear face and propagating toward the impacted surface as impact energy was increased. Wu and Springer[6] rationalized their claim that delamination is caused by opposing normal forces because the Mode I fracture toughness (G_{Ic}) for composite materials' interfaces is generally quite small. In an analysis performed by Yarve[8], impact generated tensile waves in excess of three times the laminate's ultimate through-the-thickness strength ($\sigma_{zz\ ult}$) were reported. The tensile σ_{zz} generated from the reverse curvature appeared more widespread and significant than τ_{xz} stresses. If matrix cracks were caused by shear and were required for delamination to occur, the σ_{zz} (already present) is expected to create delamination.

When a composite panel is impacted by a low velocity nonpenetrating projectile, a compressive wave is developed within the laminate. This stress wave propagates through the thickness and when reaching the rear face boundary, is reflected back as a tensile wave. For very low energy impacts, the tensile wave is believed to have sufficient amplitude to delaminate one or two of the rear face plies. With higher energy nonpenetrating impacts, several more plies (beginning at the rear face) are delaminated[4]. Graphite/epoxy laminates impacted by penetrating spherical projectiles exhibit two primary fracture modes. Damage sustained on the laminate's front face resembles a cleanly cut shear plug. Damage sustained near the laminate's rear face is extreme delamination several times the projectile's diameter[9,10]. As shown in Figure 1a, laminate penetration at velocities just above the V_{50} (a velocity where 50% of the projectiles are expected to penetrate the target) often results in rear face delaminated material (having little stiffness) being pushed aside by the projectile, only to rebound forming a closed hole. At higher impact velocities, the fiber's inertia does not allow sufficient flexure, so open holes through the laminate can be obtained. (See Figure 1b.)

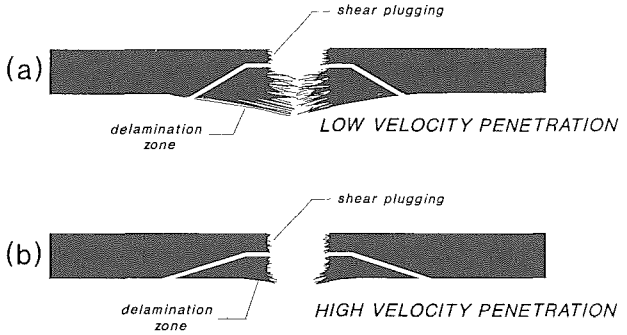

Figure 1. Dual Mode Fracture Damage for Low and High Velocity Impacts

This study investigates validity of the hypothesis that the transition from shear plugging to delamination occurs when the laminate's tensile wave is overpowered by a localized zone of compressed material which precedes the projectile through the laminate. When a nonplanar (spherical) projectile first contacts the laminate, two compressive stress waves are generated simultaneously. One wave propagates into the laminate and the other is attenuated within the projectile. The laminate's wave is expected to have

a velocity based on the material's modulus and density. With the possible exception of matrix microcracking caused by the high rate of loading, insignificant damage is created by the laminate's compressive wave. As propagation continues, the laminate's wave is eventually reflected off the free surface and returns as a tensile wave. Tensile forces applied normal to the laminate are expected to result in delamination. Because the tensile wave is initiated adjacent to the laminate's rear face and propagates toward the impacted surface, so too will the delaminations.

Energy associated with the tensile wave is attenuated with wave dilatation and as work is performed during the delamination process. With energy attenuation, the magnitude of delamination generated on each interface decreases proportionately, but remains influenced by the stiffness mismatch. The laminate's tensile wave amplitude is fully attenuated upon coincidence with the localized compression zone formed in front of the projectile. Any release wave transferred from a non-planar projectile to the laminate is not expected to significantly change the amplitude of the locally compressed material preceding the projectile. The tensile wave/compression zone interaction should create a well defined plane where a transition of fracture modes occurs from shear plugging to delamination. With continued penetration, the projectile passes through the transition plane and into the delaminated zone. Resistance to penetration therefore changes based on the new material state being penetrated.

At very high velocities, the shearing process is expected to continue through the delaminated plies (as was illustrated in Figure 1b), but without affecting the transition plane's position. Shearing through previously delaminated material at high velocities is expected to result in insignificant additional structural damage.

Stress Wave Propagation

For the one-dimensional case, the stress wave velocity (c_L) is solely a function of the material's density (ρ) and elastic modulus (E) in the wave direction (equation 1), whereas Poisson's ratio (μ) is included in the three-dimensional case (equation 2)[17].

$$c_L^2 = \frac{E(g)}{\rho} \quad \text{(one-dimension)} \tag{1}$$

$$c_L^2 = \frac{E(1-\mu)(g)}{\rho(1+\mu)(1-2\mu)} \quad \text{(three-dimension)} \tag{2}$$

Note: Acceleration due to gravity (g) is included.

The transverse (through-the-thickness) stress wave velocity generated within a plate (as a result of normal impact) is most accurately described according to equation 2. If fibers are present in the matrix, micro-impedance differences are expected to influence the stress wave's velocity, amplitude, and length.

In this study, through-transmission (an ultrasonic NDI technique) was used to obtain the wave's transverse velocity so that an effective through-the-thickness modulus could be calculated. Sound velocity measurements were obtained through the thickness of monolithic 8, 16, 32, 48, and 64-ply laminates. All specimen thicknesses exhibited a transverse wave velocity of 118,000 in/s (3 km/s). (This correlates well with through-the-thickness stress wave velocities of 114,200 in/s (2.9 km/s) measured by Dutta[18], but differs slightly from the 92,900 in/s (2.36 km/s) suggested by Kim and Moon[19] and the 139,400 in/s (3.54 km/s) suggested by Yarve[8].) With the density of the AS4/3501-6 laminate being 0.055 lb/in^3[3], the elastic modulus in the z-direction was calculated according to equation 3,

$$E_z = \frac{\rho(c_L^2)}{g} \tag{3}$$

$$E_z = \frac{(0.055)\ (118{,}000^2)}{386.4}$$

$$E_z = 1.982 \text{ msi}$$

where E_z is the transverse modulus in lbs/in^2, ρ is the density in lbs/in^3, c_L is the wave velocity in in/sec, and g is the acceleration due to gravity in in/sec^2.

If the depth of the localized compression zone in front of the projectile is ignored, and one assumes the fracture mode transition plane is formed by an interaction between the laminate's tensile wave and the projectile, the following equation can be used to determine a lower bound depth for the transition plane:

$$z = \frac{v_p\ (2t - z)}{c_L} \tag{4}$$

where z is the distance from the laminate's impacted surface to the proposed change in fracture modes, v_p is the average projectile velocity (in the laminate) until the tensile wave is encountered, t is the laminate's thickness, and c_L is the laminate's stress wave velocity (assumed constant in both tension and compression).

II. Objective

The objective of this study was to determine the basis for delamination initiation and propagation within a laminate impacted at high velocity. The primary goal was to establish and support an explanation for fracture mode transformation along the projectile's path.

III. Approach

In this study, a series of instrumented graphite/epoxy composite laminates are impacted by steel spherical projectiles at 1300, 1850, and 2380 f/s. These velocities are above the 32-ply laminate's V_{50} of 375 f/s and 128-ply laminate's V_{50} of 1267 f/s. Although several external dynamic measurements are made, imbedded within the targeted laminates are an alternating series of stress and strain gages to monitor the diverging stress wave. Rear face panel deflections are recorded optically during the impact event and are correlated with stress events. Post-mortem investigations are limited to C-scans and are used to correlate fracture modes with data recorded during the impact event. Stress, strain, displacement, and NDI data are used to evidence the source of delamination initiation and propagation. Delamination is assumed to occur simultaneously with tensile stress output. The transverse stress wave together with a combination of the wave's dilatational component and Poisson's effects are recorded. Tensile wave attenuation is correlated with the on-coming projectile's localized compression front and used to predict the location of the fracture mode transition from shear plugging to that of delamination.

The composite material used throughout this study was graphite/ epoxy (AS4/3501-6). Two quasi-isotropic laminate thicknesses (32-ply and 128-ply) were employed to assist in determining flexure effects on delamination. Although the quasi-isotropic 32-ply lay-up $[(0/90/+45/-45)_4]_s$ was held

constant, two different panel configurations were established. Monolithic laminates (0.185-inch thick and fabricated in one step) were used during control experiments. For stress wave experiments, the 32-ply laminates consisted of four unbalanced unsymmetric sublaminates post-bonded together (after sensor installation on each of the three interfaces). Similarly, 128-ply $[(0/90/+45/-45)_{16}]_s$ laminates consist of eight sublaminates with sensors on each of the seven interfaces.

Specimen Dimensions and Boundary Conditions

All test specimens measured 8x8 inches. The dimensions were chosen to ensure radial wave propagation and reflection did not interfere with through-the-thickness stress wave measurements. Specimens were clamped around the periphery, yielding a 7x7-inch free surface. Actual edge conditions provided by the fixture were assumed to fall between fully clamped and simply supported. Care was taken to ensure an equal degree of clamping, even though previous researchers[15,16,20] found that boundary conditions sufficiently remote from the point of impact do not influence the damage state.

Specimen Bondlines

Ideally, sublaminate bondlines would have mechanical properties identical to the 3501-6 resin; however, temperature limitations of the imbedded sensors required that a room temperature curing epoxy be used. The non-toughened system selected was Hysol's RE2039 epoxy with HD3719 hardener (mixed at a 1:1 ratio). Except for impact generated disbonds, the bondlines were assumed not to influence delamination excessively.

Projectile

All tests were performed using a 0.5-inch chromium steel sphere having a density of 0.284 lb/in^3 (7.9 g/cm^3) and modulus of 30 msi. Spherical projectiles were chosen for this study to produce a high-amplitude short-duration wave front. Although simple spheres do not possess the complex geometry of threats commonly encountered in battlefield environments, spheres provide the necessary uniformity for repeatable testing while maintaining projectile/target interactions similar to those generated by typical blunt projectiles.

Specimen Instrumentation and Data Acquisition

In an attempt to differentiate between radial and transverse wave amplitudes, carbon stress gages (relatively insensitive to in-plane stresses) and constantan strain gages (relatively insensitive to normal stresses) were chosen for the study. (Carbon stress gages had an active area of 0.05 x 0.06 inch, whereas the active area of constantan strain gages was 0.1 x 0.1 inch.) Stress gages were capable of recording compression amplitudes only. Although stress gages also provid tensile output, this data was not capable of being calibrated. Strain gages were calibrated for recording tension and compression data. All gages were dispersed throughout each panel in an alternating fashion (Figure 2) and used to track the stress wave's progress.

Common to both 32 and 128-ply laminates were midplanes containing strain gages. Data from these gages were free from flexure effects and therefore provided a direct observation of the stress wave's dilatation and Poisson's effects. Flexure data was obtained via a non-contact fiber optic means. To avoid damaging the fiber optic wand, the sensor was positioned 1.5 inches off-center from the shotline as shown in Figure 3.

Stress and strain data were acquired at a 50 MHz sampling rate with 8-bit resolution. Displacement data were acquired at 200 KHz. The lower sampling rate for displacement was a function of the integral fiber optic device. Displacement data was recorded real-time into an open 20 MHz channel on the data acquisition system. Doing so allowed time-wise correlation of displacement data with stress and strain data.

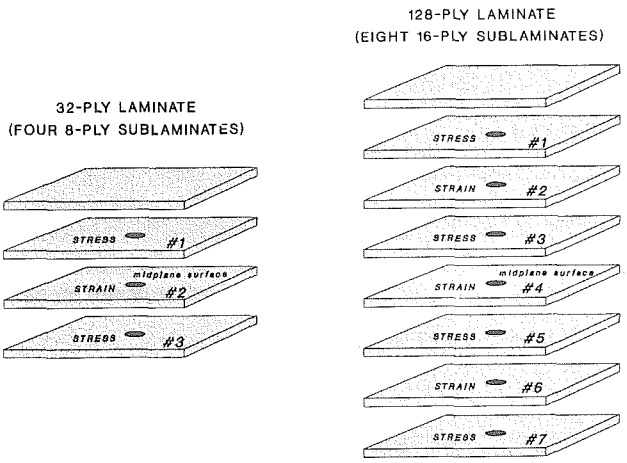

Figure 2. Gage Stacking Sequence Within 32 and 128-Ply Laminates

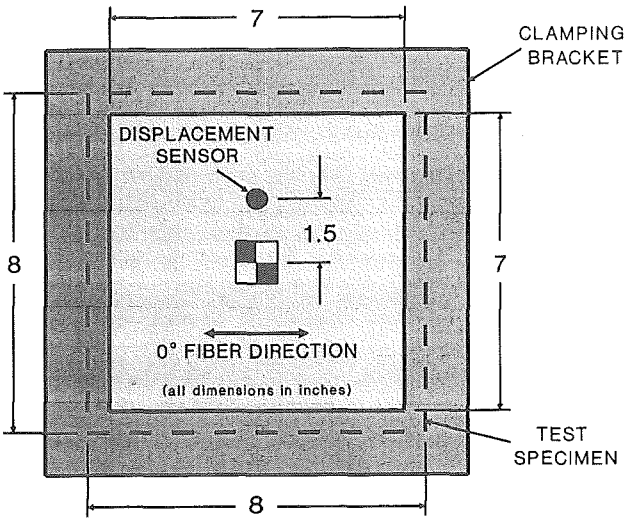

Figure 3. Location of Rear Surface Displacement Sensor

The data acquisition system was triggered by the projectile severing a pencil lead trigger adjacent to the laminate. Upon being triggered, 256,000 data points (divided such that 28% were before the trigger) were recorded by each channel. Simultaneously (using the same trigger), the pulsed power supply sent a 120 μ-sec square wave voltage to each of the embedded sensors. Timing was obviously critical.

Test Setup and Experimental Procedures

The test fixture consisted of a steel box beam to which a clamping assembly was welded. Three built-in shims (ledges) were used to consistently register the location of the test specimen's lower left corner. To achieve the desired impact accuracy of ±0.04-inch (1mm) (required to ensure direct contact with the embedded gages) the gas gun muzzle was positioned two feet from the specimen. The shotline was oriented perpendicular to the specimen's surface and passed directly through the stack of embedded instrumentation. (See Figure 4.)

Post-mortem investigations were limited solely to time-of-flight C-scans. The NDI technique was used to observe the fracture mode transition by identifying the depth of the delamination interface closest to the impacted surface.

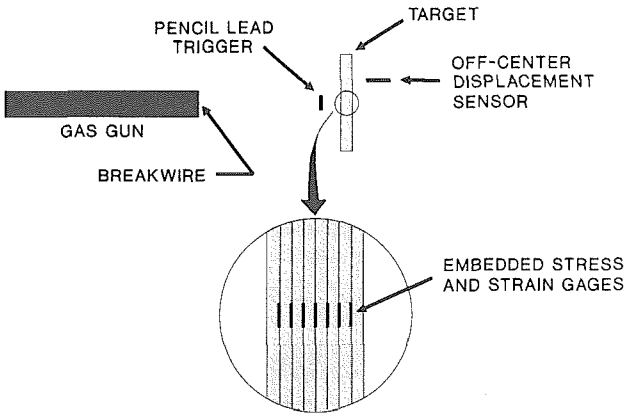

Figure 4. Shotline through the Imbedded Instrumentation

IV. Stress Wave Experiments

Specimens tested, along with flexure and stress wave velocity results are shown in Table 1. The time difference between the estimated time-of-contact and initial flexure recorded by the off-center displacement sensor was used to obtain the flexure wave velocity. Flexure wave velocities varied between 862 and 1666 f/s and generated a maximum displacement at the off-center location of 0.027-inch. Substantial differences in the flexure wave velocities were believed the result of difficulties in detecting flexure initiation.

The stress wave velocity proved much more capable of generating damage early in the impact event. This point is illustrated in Figure 5 using data similar to that which was measured. A tensile stress wave (reflected from the rear surface) has sufficient amplitude to create delamination within the first few microseconds. Flexure, on the other hand, remains insignificant during this period. (Note: The flexure slope plotted was not measured during the time frame shown, but represents the maximum slope recorded later in the impact event.)

TABLE 1. Impact Tests Performed on Instrumented Laminates Using a 0.5-Inch Diameter Steel Projectile

PANEL NO.	PANEL THK. (plies)	IMPACT VEL. (f/s)	FLEX. WAVE VELOCITY (f/s)	MAXIMUM DISPLACEMENT (in)	TRANSVERSE STRESS WAVE VELOCITY (in/s)
D13.1	128	2380	910	-	120,888
B9.1	32	2380	1238	0.025	-
B8.3	32	2380	1600	0.020	-
B1.3	32	2380	862	0.018	-
D7.1	128	1850	967	-	125,822
D10.1	128	1850	-	-	-
B2.3	32	1850	1666	0.015	-
D14.1	128	1300	-	-	117,121
B10.3	32	1300	1057	0.027	-

Stress wave velocity calculations are based strictly on the initial response of each stress gage. An example of this (based on specimen D13.1) is shown in Figure 6. Active stress gages were mounted in positions 1 and 7, whereas strain gages were in positions 2, 4, and 6. Strain gages did not respond immediately to the stress wave's passing, presumably due to the low amplitude in-plane signal generated. Stress wave velocity measurements of 120,888 in/s, 125,822 in/s, and 117,121 in/s correlate well with the 118,000 in/s acoustic wave velocity reported earlier. Based on the measured (or typical) stress wave velocities, the projectile's time-of-contact was estimated for each of the laminates tested.

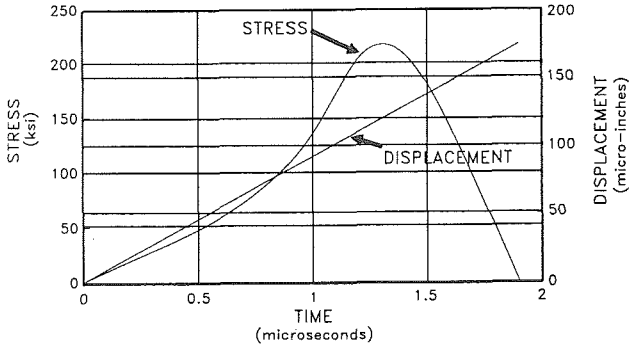

Figure 5. Stress Wave Amplitude Vs Flexure Amplitude Early in the Impact Event

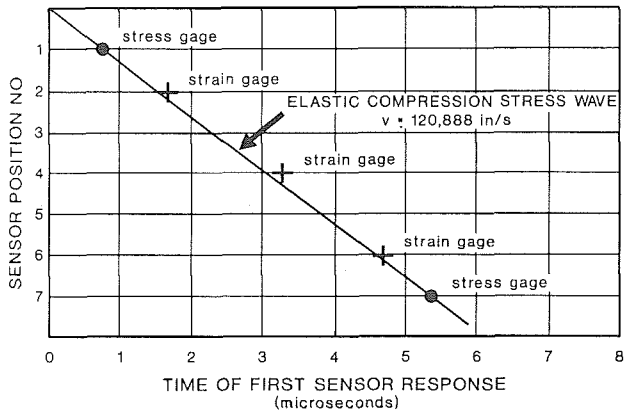

Figure 6. Stress Wave Velocity Based on First Sensor Response Times (Panel D13.1)

Transverse Stress Wave Amplitude Measurements

Figure 7 shows typical stress gage output (although this data curve is peculiar to specimen D14.1, stress gage position 1). The estimated time-of-contact, based on the first stress gage response and a stress wave velocity of 117,121 in/s (as measured from point B), is identified by point A (t = 0). Note that even though the gage is powered, the output voltage remains at zero until contacted by the stress wave. The first stress gage response occurs at point B (t = 0.83 μ-sec). Maximum out-of-plane compression produced by the passing stress wave is identified by point C (σ = -206 ksi). The significant increase in compression stress (indicated by point D, t = 3.18 μ-sec) is believed the result of a localized zone of compressed material which precedes the projectile through the laminate. The fastest time the projectile could arrive at the gage to ensure failure (based on a rigid specimen and an initial projectile velocity of 1296 f/s) is identified by point E, t = 6.21 μ-sec. With this position 1 gage location being so far from the rear surface, stress output is not affected when the returning tensile stress wave is scheduled to arrive (point F, t = 12.38 μ-sec). The slowest time that the projectile would arrive at the gage to insure failure (based on a rigid specimen and a residual projectile velocity of 275 f/s) is marked by point G, t = 29.28 μ-sec. Note that the gage failure (a continuous rise to significant tensile output) does in-fact occur between points E and G.

Figure 8 illustrates the relationship between the compression stress wave amplitudes and depths (z-direction) for each of the three impact velocities. (Depth is measured from the point-of-impact.) Although data scatter is present (primarily for the 1850 f/s velocity), stress wave amplitudes are attenuated with increased depth and decreased velocity.

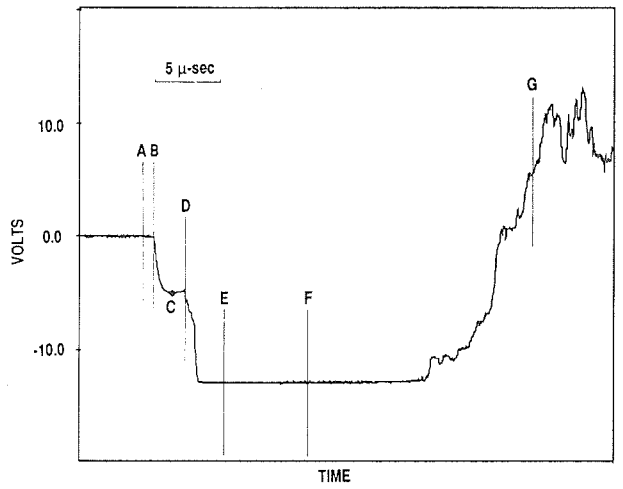

Figure 7. Typical Stress Gage Output (Specimen D14.1, Stress Gage Position 1)

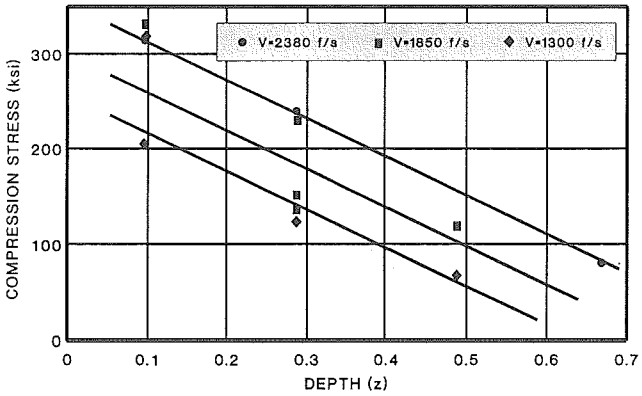

Figure 8. Compression Stress Wave Amplitude Vs Depth for Three Impact Velocities Above the V_{50}

In-Plane Strain Measurements

Figure 9 shows typical strain output (although this data curve is peculiar to specimen D14.1, strain gage position 6) in greatly expanded form. The estimated time-of-contact based on the first stress gage response (position 1) is indicated by point A (t = 0). Point B marks the initial strain gage response (t = 5.28 μ-sec). The maximum in-plane tensile amplitude (ε = 0.008) produced by the passing compression stress wave is indicated by point C. Point D is the estimated time-of-arrival for the return tensile wave based on a stress wave velocity of 117,121 in/s (t = 8.25 μ-sec). The in-plane strain amplitude at point E is roughly equivalent (but opposite in sign) to that at point C. Gage failure is indicated by the sudden tensile strain at point F (t = 30.48 μ-sec).

Note that with arrival of the tensile wave, the strain changes quickly from tension to compression. This change of sign indicates Poisson's effects play a significant role in the generation of in-plane strains. (If dilatational effects were significant, the in-plane strain would remain tensile). Because the strain amplitude is maintained (after the sign change), suggests the return tensile stress wave amplitude (an otherwise unknown value) is approximately equal to that of the original compression wave. With the transverse tensile strength ($\sigma_{zz\ ult}$) of AS4/3501-6 estimated to be 7 ksi[8], and tensile stress amplitudes identical to that of compression, the tensile stress has ample opportunity to generate fracture early in the impact event.

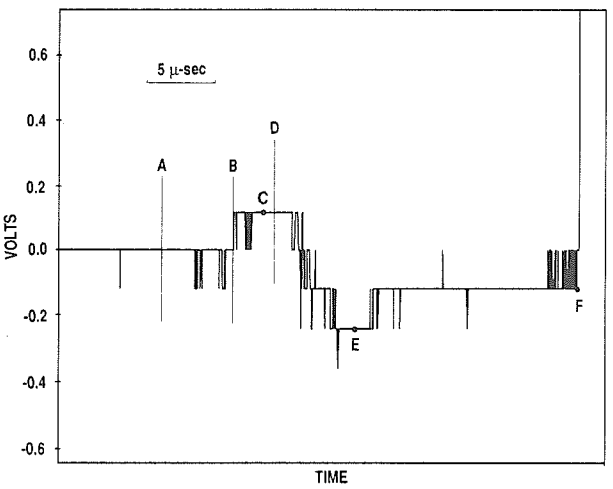

Figure 9. Typical Strain Output (Specimen D14.1, Strain Gage Position 6)

Fracture Mode Transition

Significant disbonds along the three bondlines in the 32-ply laminates, and 7 bondlines in the 128-ply laminates, precluded observation of the fracture mode transition via NDI techniques. It proved convenient, however, to observe the fracture mode transition via NDI of the monolithic specimens. An example NDI cross section (panel E78-3, having an impact velocity of 1014 f/s) is presented in Figure 10. The apparent transition from shear plugging to delamination occurs at a depth of 0.046-inch. The

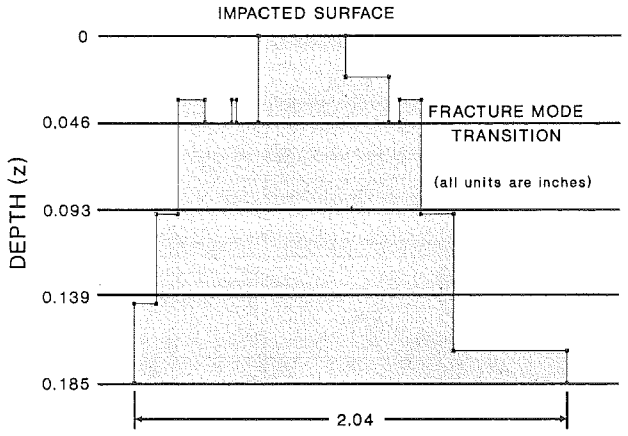

Figure 10. Cross Section of Through-the-Thickness Damage Sustained by Panel E78-3, a 32-Ply Monolithic Laminate Impacted by a 0.5-Inch Diameter Steel Sphere at 1014 f/s

z-t diagram (Figure 11) for projectile interaction with the stress wave indicated the transition should have occurred at a depth of 0.034-inch. [Note: The predicted depth, also solved via equation 4, is based on the projectile's preimpact (initial) velocity because the transition occurs so near the impacted surface.] The deeper actual transition is believed the result of a localized compression zone which precedes the projectile through the laminate. Based on the times at which gages (of known depth) were influenced by this compressed material (refer back to point D in Figure 7) and the estimated projectile depth, the thickness of the compression zone was quantified. (See Figure 12.) (Although not identified in Figure 12, the compression zone thickness appeared to be independent of the impact velocity.) The estimated compression zone thickness (based on a projectile depth of 0.034-inch and an

extrapolation of data in Figure 12) is 0.025-inch. When coupled with the projectile's depth, the returning tensile wave can be effectively overpowered at a depth of 0.059-inch. With the fracture mode transition occurring at 0.046-inch (between the lower and upper bounds of 0.034 and 0.059-inch) the hypothesis appears accurate.

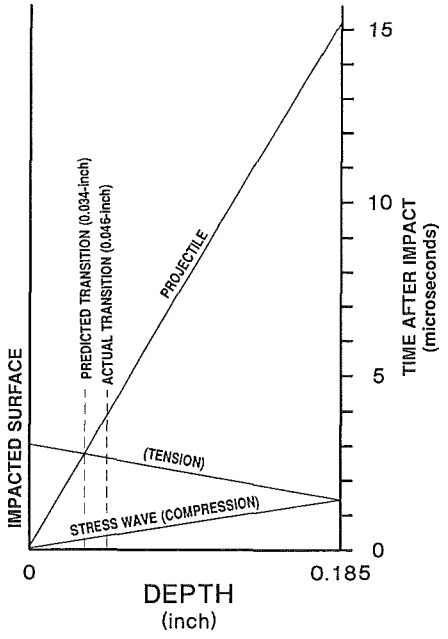

Figure 11. Z-T Diagram of the Tensile Return Wave's Interaction with the Projectile (Panel E78-3)

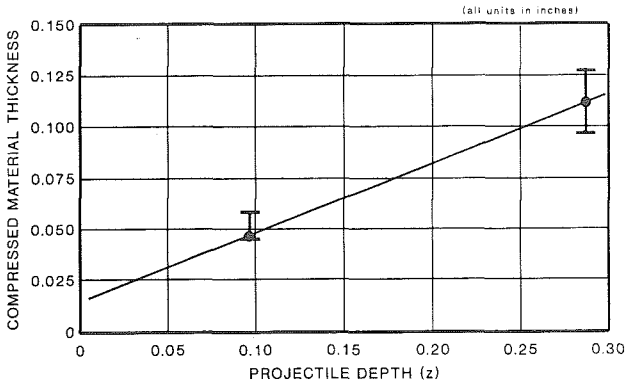

Figure 12. Projectile Depth Vs Compression Zone Thickness

V. Summary and Conclusions

An experimental procedure was developed to observe transverse stress wave propagation through impacted composite laminates. Impact experiments were performed on instrumented graphite/epoxy (AS4/3501-6) laminates in an effort to determine the basis for delamination initiation and propagation. In doing so, an explanation for the fracture mode transformation from shear plugging to delamination was established. When high-velocity steel spheres (0.5-inch diameter) impacted quasi-isotropic laminates, transverse stress wave propagation was recorded by the imbedded stress and strain sensors to have progressed through the laminate and reflected at the rear surface. The tensile wave is identified to have sufficient energy to initiate and propagate delamination from the rear surface toward the point of impact. The tensile wave was also demonstrated to have been attenuated by locally compressed material preceding the projectile. Inspection of time-of-flight C-scans revealed a correlation between the predicted location of tensile wave attenuation and the last interface delaminated. An adjustment to the method of prediction (which accounts for the localized compression zone ahead of the projectile) lends itself to an accurate explanation for the fracture mode transition from shear plugging to delamination. The transition from shear plugging to delamination is therefore identified to occur when the localized compression front (associated with the projectile) interacts with the tensile wave.

References

1. Cantwell, W.J., P.T. Curtis, and J. Morton, "Impact and Subsequent Fatigue Damage Growth in Carbon Fibre Laminates", International Journal of Fatigue, Vol. 6, No. 2, April 1984, pp 113-118.

2. Avery, W.B., and D.H. Grande, "Influence of Materials and Layup Parameters on Impact Damage Mechanisms", 22nd International SAMPE Technical Conference, November 1990, pp 470-483.

3. Husman, G.E., J.M. Whitney, and J.C. Halpin, "Residual Strength Characterization of Laminated Composites Subjected to Impact Loading", Foreign Object Impact Damage to Composites, ASTM STP 568, American Society for Testing and Materials, 1975, pp 92-113.

4. Foos, B.C., "Damage Progression in Composite Plates Due to Low Velocity Impact", Thesis, Dept. of Civil Engineering, Ohio State University, 1990.

5. Gosse, J.H. and P.B.Y. Mori, "Impact Damage Characterization of Graphite/Epoxy Laminates", Proceedings of the American Society for Composites, 3rd Technical Conference on Composite Materials, September 1988, pp 344-353.

6. Wu, H.T. and G.S. Springer, "Impact Induced Stresses, Strains, and Delaminations in Composite Plates", Journal of Composite Materials, Vol. 22, June 1988, pp 533-560.

7. Evans, K.E. and N.J. Herne, "The Prediction of Damage Due to High Velocity Impact in Composite Laminates", Computer Aided Design in Composite Material Technology, Proceedings of the

International Conference, Southhampton, England, April 1988, pp 383-393.

8. Yarve, E.V., "Dynamic Response of Composite Plates to Impact Load", Contract F33615-88-C-5420, Task 20, Wright-Patterson AFB, May 1991.

9. Vasudev, A., K. Okajima, and S.J. Bless, "Effects of the Transverse Strength and the Density on the Penetration Mechanism of Thick Glass-Fiber-Reinforced-Plastics", March 1987.

10. Cristescu, N., L.E. Malvern, and R.L. Sierakowski, "Failure Mechanisms in Composite Plates Impacted by Blunt-Ended Penetrators", Foreign Object Damage to Composites, ASTM STP 568, 1975, pp 159-172.

11. Cordell, T.M. and P.O. Sjoblom, "Low Velocity Impact Testing of Composites", Proceedings of the American Society of Composites, First Technical Conference, October 1986, pp 297-312.

12. Boll, D.J., W.D. Bascom, J.C. Weidner, and W.J. Murri, "A Microscopy Study of Impact Damage of Epoxy-Matrix Carbon-Fibre Composites", Journal of Materials, Vol. 21, August 1986, pp 2667-2677.

13. Dost, E.F., L.B. Ilcewicz, and J.H. Gosse, "Sublaminate Stability Based Modeling of Impact-Damaged Composite Laminates", Proceedings of the 3rd Technical Conference on Composite Materials, American Society for Composites, September 1988, pp 354-363.

14. Liu, D., "Impact-Induced Delamination - A View of Bending Stiffness Mismatching", Journal of Composite Materials, Vol. 22, July 1988, pp 674-692.

15. Liu, D. and L.E. Malvern, "Matrix Cracking in Impacted Glass/Epoxy Plates", Journal of Composite Materials, Vol. 21, July 1987, pp 594-609.

16. Kandalaft, I.F., "Visible Damage in Impacted Composite Plates", Masters Thesis, Ohio State University, 1990.

17. Zukas, J.A., T. Nicholas, H.F. Swift, L.B. Ggreszczuk, D.R. Curran, "Impact Dynamics", John Wiley and Sons, New York, 1982.

18. Dutta, P.K., D. Hui, A. Mayer, and G. Czarnecki, "Stress Wave Propagation Through the Thickness of Laminated Plates Using PVDF Sensors", Technical Note, US Army Cold Regions Research and Engineering Laboratory, July 1991.

19. Kim, B.S. and F. Moon, "Impact Induced Stress Waves in an Anisotropic Plate", AIAA Journal, Vol. 17, No. 10, October 1979, pp 1126-1133.

20. Wu, H.T. and G.S. Springer, "Measurements of Matrix Cracking and Delamination Caused by Impact on Composite Plates", Journal of Composite Materials, Vol. 22, June 1988, pp 518-532.